Title

Evolutionary processes and its environmental correlates in the cranial morphology of western chipmunks (Tamias).

Journal

Evolution; international journal of organic evolution, 71(3)

ISSN

0014-3820

Authors

Assis, Ana Paula A
Rossoni, Daniela M
Patton, James L
et al.

Publication Date

2017-03-01

DOI

10.1111/evo.13137

Peer reviewed

doi:10.1111/evo.13137

Evolutionary processes and its environmental correlates in the cranial morphology of western chipmunks (*Tamias*)

Ana Paula A. Assis,[1,2] Daniela M. Rossoni,[1] James L. Patton,[3] and Gabriel Marroig[1]

[1]*Department of Genetics and Evolutionary Biology, Biosciences Institute, University of Sao Paulo, Sao Paulo 05508-900, Brazil*

[2]*E-mail: paulaaprigio@usp.br*

[3]*Museum of Vertebrate Zoology, Department of Integrative Biology, University of California, Berkeley, California 94720*

Received November 3, 2015
Accepted November 2, 2016

The importance of the environment in shaping phenotypic evolution lies at the core of evolutionary biology. Chipmunks of the genus *Tamias* (subgenus *Neotamias*) are part of a very recent radiation, occupying a wide range of environments with marked niche partitioning among species. One open question is if and how those differences in environments affected phenotypic evolution in this lineage. Herein we examine the relative importance of genetic drift versus natural selection in the origin of cranial diversity exhibited by clade members. We also explore the degree to which variation in potential selective agents (environmental variables) are correlated with the patterns of morphological variation presented. We found that genetic drift cannot explain morphological diversification in the group, thus supporting the potential role of natural selection as the predominant evolutionary force during *Neotamias* cranial diversification, although the strength of selection varied greatly among species. This morphological diversification, in turn, was correlated with environmental conditions, suggesting a possible causal relationship. These results underscore that extant *Neotamias* represent a radiation in which aspects of the environment might have acted as the selective force driving species' divergence.

KEY WORDS: **Climatic niche, morphometrics, natural selection, quantitative genetics, phylogenetic comparative methods.**

Understanding the role of separate evolutionary processes in driving phenotypic diversification and shaping the way species interact with their environment has been a central concern in biology. Numerous theoretical advances show that even very divergent phenotypes could evolve through a neutral process of genetic drift (Lande 1979; Pie and Weitz 2005; Stayton 2008). Therefore, rather than simply assuming that species have diversified adaptively, the initial step in any study should be one that tests if a random evolutionary process could generate the observed phenotypic diversity. Moreover, to understand how species diversify and adapt to different environments is essential, especially in a world threatened by human induced changes. One major factor influencing species' phenotypic evolution is climate (Barnosky et al. 2003), which is also one of the major aspects influenced by human actions (IPCC 2014). Therefore, by studying a group of species that diversified recently to occupy a wide range of climatic niches we can gain a better understanding of how climate change might impact species evolution.

The western North American chipmunks, genus *Tamias*, subgenus *Neotamias*, comprise 23 extant species that originated about ~2.75 million years ago in the early Pleistocene (Reid 2006; Sullivan et al. 2014). This clade is one of the most speciose among North American mammals and exhibits the hallmarks of a recent, rapid radiation (Good et al. 2003; Reid et al. 2012; Sullivan et al. 2014). In striking contrast, the sister group to *Neotamias* includes two lineages, neither of which has apparently undergone any speciation event since their respective origins: *Tamias sibiricus* (subgenus *Eutamias*) is distributed through a large geographic region in temperate Asia, and *Tamias striatus* (subgenus *Tamias*) occurs throughout the eastern United States and adjacent Canada. Species of *Neotamias* are ubiquitous members of the diverse

This article corresponds to Jeremy C. R. (2017), Digest: Climate effects on chipmunk cranial morphology. Evolution. DOI:10.1111/evo.13185.

EVOLUTION
INTERNATIONAL JOURNAL OF ORGANIC EVOLUTION

habitats found across western North America, which include alpine tundra, all types of conifer and western hardwood forests, sagebrush plains, brush covered montane slopes, and dense temperate rainforest (Nowak 1999), biomes that span an elevational gradient from sea level to 4000 meters and an environmental gradient from coastal humid areas to the dry intermontane interior (Johnson 1943; Reid 2006). As many as seven species may be found along a single elevational transect, as in the central Sierra Nevada in California (Grinnell and Storer 1924), with up to four species co-occurring in a single area (Sullivan et al. 2014). Nevertheless, conspicuous niche partitioning is apparent in multispecies assemblages and sharp elevational zonation patterns are typical, resulting in limited true syntopy (Grinnell and Storer 1924; Heller 1971; Heller and Gates 1971; Heller and Poulson 1972; Bergstrom 1992).

We chose to study the skull in these chipmunks because it is one of the most important structures determining how mammalian species perceive and interact with their environment. In this way, we hope to gain a better understanding of how these chipmunks adapted and diversified to their strikingly different environments. Beyond the obvious role that the jaws and teeth play in food acquisition and initial processing, the interconnected bony elements of the skull serve to protect the brain and sensory organs (eye, inner ear, olfactory receptors; Elbroch 2006) and serve in water balance and temperature regulation (counter-current water and heat exchange via the nasal passages and convoluted turbinal bones; Schmidt-Nielsen et al. 1970). Among mammals, rodents exhibit a great array of feeding specializations, with their characteristic single pair of gnawing incisors and highly specialized masticatory muscles hypothesized to underlie their extreme evolutionary success (Cox et al. 2012). Moreover, several studies have suggested that cranial trait differences among chipmunk species resulted from their response to environmental conditions associated with the differential habitats occupied (Allen 1890; Patterson 1980, 1983; Sutton and Patterson 2000). Such striking features make this group a good model for examining underlying evolutionary processes.

Herein, by using phylogenetic comparative methods within the framework of quantitative genetics theory, we examined the pattern of variation in quantitative attributes of the chipmunk skull. Our goal was to disentangle the relative roles of genetic drift and selection in their cranial phenotypic evolution and relate this to possible selective pressures. We started by testing hypotheses of evolutionary diversification in *Neotamias*, to understand if the cranial diversity seen among species could be explained solely by genetic drift, natural selection, or a combination of these two processes. We then investigated if climatic variables (potential selective agents) are associated with the evolution of morphological traits, which would be expected under natural selection. The phenotype-environmental correlation is thought to be an essential part of the adaptation process and one of the aspects that can demonstrate an adaptive radiation (Wainwright and Reilly 1994; Schluter 2000). Therefore, understanding how cranial traits are correlated with environmental variables might enlighten us on how ecological variation can promote divergence between species (Wainwright and Reilly 1994).

Methods

SAMPLE AND MEASUREMENT

We measured 2238 skulls representing 20 of the 23 species of *Neotamias* and the single species in the subgenus *Tamias* (*T. striatus*) (taxa and sample sizes available in Table S1). All specimens are deposited in the Museum of Vertebrate Zoology (MVZ, Berkeley, CA) and National Museum of Natural History (NMNH, Washington, DC). We included only adult specimens, defined by full eruption of the permanent premolar 4 and a completely fused basisphenoid-basioccipital suture. The taxonomic arrangement used throughout this study follows Wilson and Reeder (2005), and the phylogeny presented is based on Sullivan et al. (2014). For polytypic species we included only a single representative subspecies. In a few cases where specimen availability was limited (see Table S1), we included individuals assignable to two subspecies. We removed significant differences due to sex, locality, subspecies, and age (adults divided in three categories defined by tooth wear: (1) no signs of wear, (2) moderate signs of wear and (3) extensive signs of wear), prior to the estimation of the pooled within-species phenotypic variance/covariance (V/CV) matrices, using the residuals of a multivariate analysis of variance (MANOVA), and a pooled-by-subspecies mean was used for each trait (Table S1).

One of us (APAA) recorded three-dimensional coordinates for 27 landmarks on each skull (Fig. 1; Table S2) using a Microscribe 3D MX digitizer (Microscribe, IL). Landmarks were positioned at the intersection of sutures or other discrete (and homologous) cranial features; each landmark was readily identifiable in all specimens. We chose this set of landmarks to reflect potentially important developmental and functional relationships among cranial structures while simultaneously representing the whole skull (Cheverud 1982; Marroig and Cheverud 2001). A set of 38 linear measurements was then calculated from the landmark coordinates (Fig. 1); these typically encompass only a single bone of the skull and thus capture localized developmental/functional processes. Bilaterally symmetrical measurements were averaged, and if the skull was damaged on one side, the other was used instead of the average. All specimens were measured twice, allowing the estimation of repeatability to account for measurement error (Lessels and Boag 1987). The average of repeated measurements was used in all subsequent analyses. Here, we chose to use a traditional morphometric approach because most of our analyses

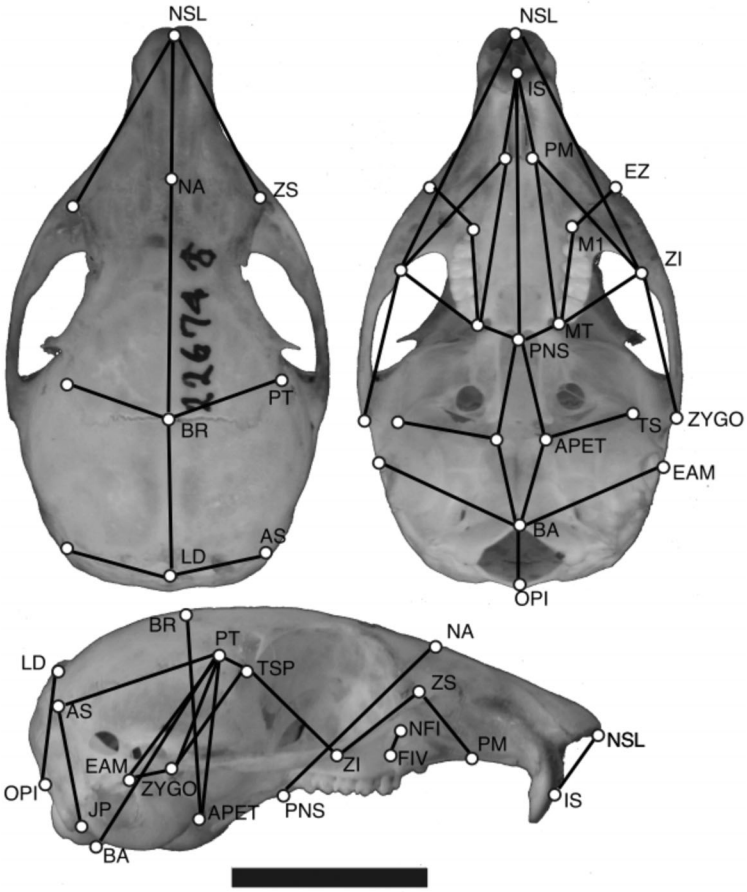

Figure 1. **A skull of *T. alpinus* displaying the landmarks and linear measurements used in the study. The scale bar = 1 centimeter. A brief description of each landmark position is available in Table S2.**

are dependent on the estimation of covariance between traits. To do this within the framework of geometric morphometrics would require much larger sample sizes, beyond the availability of specimens in the visited museums (at least three times the number of landmarks; Zelditch et al. 2004). Moreover, local variation among landmarks is not necessarily preserved in covariance matrices obtained through a Procrustes Superimposition procedure (Linde and Houle 2009; Adams et al. 2013).

GENETIC DRIFT TESTS

We applied two different drift tests to evaluate which evolutionary process was responsible for the cranial diversity observed among *Neotamias* species. Both are based on quantitative genetics predictions for groups evolving through drift (Lande 1979; Ackermann and Cheverud 2002; Hohenlohe and Arnold 2008). The first is referred as a regression test and the second as a principal components (PCs) correlation test. Both tests are based on the premise that the species patterns of covariance have remained relatively stable throughout their diversification. To verify this premise, we compared phenotypic covariance matrices (**P**-matrices) among species using Random Skewers and Krzanowski methods (Krzanowsky 1979; Blows et al. 2004; Cheverud and Marroig 2007). Moreover, we also compared **P**-matrices with a **G**-matrix derived from a distant-related rodent species (*Akodon cursor,* Porto et al. 2009). We found considerable similarity in the covariance structure for all matrices using both methods (see Supplementary Material for further discussion; Tables S3 and S4 and Fig. S1). These results allowed us to continue with the investigation of the evolutionary processes responsible for the diversification of *Neotamias*.

Regression test: Proposed by Ackermann and Cheverud (2002), the idea behind this test is that in populations evolving through genetic drift the amount of observed phenotypic divergence will be proportional to the amount of variation in the ancestral population (Ackermann and Cheverud 2002; Marroig and Cheverud 2004). This relationship can be expressed by the following equation:

$$\mathbf{B}_t = \mathbf{G}\,(t/N_e)\,. \qquad (1)$$

Where $\mathbf{B}_t$ represents the V/CV matrix between groups at generation t; **G** is the additive genetic V/CV matrix of the founding

population, and N_e is the effective population size of the individual taxa (Lande 1979, 1980; Lofsvold 1988). For morphological traits, and particularly in mammalian skull studies, usually the phenotypic within-group V/CV matrix (**W**) is quite similar to **G** (Cheverud 1988; Roff 1995; Marroig and Cheverud 2001; Oliveira et al. 2009), and can therefore be used as a substitute for **G** in the above equation. This assumption of **G** and **P**-matrices exchangeability is particularly robust on empirical cases where **P**-matrices are structurally similar among species under investigation, as is the case here (see supplementary material for further discussion, Tables S3, S4). **W** can be interpreted as an estimate of the ancestral population matrix. Given that t and N_e are constant for a given comparison, the pattern of V/CV between groups (**B**) must be proportional to the V/CV pattern within groups (**W**) if the populations are evolving through genetic drift (Ackermann and Cheverud 2002, 2004; Marroig and Cheverud 2004). Alternatively, where **B** and **W** are not proportional, directional selection may have acted upon the evolution of the groups (Ackermann and Cheverud 2004; Prôa et al. 2013). To simplify this relationship of within- to between-groups variation, we transformed **W** to its principal components (PCs). On a logarithmic scale, we can write the relationship between and within groups V/CV as a linear regression:

$$\ln(\mathbf{B}) = \ln(t/N_e) + b\ln(\mathbf{W}). \quad (2)$$

In this case b corresponds to the slope of the regression line, ln(**W**) corresponds to the log transformed eigenvalues of the **W**-matrix, and ln(**B**) corresponds to the log transformed variances of the **B**-matrix. **W**-matrices were estimated for each node of the phylogeny by taking the mean over sister taxa, weighted by sample size, using the function PhyloW available in package EvolQG version 0.2–2 for R (R Core Team 2014; Melo et al. 2015). We projected the species means in the principal components of **W**, and the variance associated with each PC's projection was used as an estimate of the **B**-matrix.

If the observed diversification was due to genetic drift, we expect the slope of regression not to deviate significantly from 1.0. A significant deviation from a slope of 1.0 indicates a pattern unlikely to have been produced by drift alone (Ackermann and Cheverud 2002; Marroig and Cheverud 2004). Regression slopes above 1.0 indicate that one or more of the first few PCs are more variable, relative to the other PCs, than expected under genetic drift. This could happen through diversifying selection acting on traits contributing to the highly variable PCs and/or by stabilizing selection on the traits contributing to the later PCs. Slopes significantly smaller than 1.0 occur when species are relatively highly divergent along minor PCs. This can occur through strong diversifying selection along these dimensions and/or stabilizing selection on the remaining PCs.

Because genetic drift is rejected if the regression line between **B** and **W** deviates significantly from 1.0, the number of species involved in the analysis has an influence in the uncertainty of the confidence interval. The smaller the number of species used, the higher this uncertainty. Thus, to minimize the occurrence of type II error, we applied this analysis only to nodes with more than four descendant species. Type I error rates, on the other hand, for this test are acceptable when the diverging species satisfy the assumption of similarity in variance/covariance patterns (Prôa et al. 2013).

PCs correlation test: By definition, principal components are uncorrelated with each other. Hence, when we apply a principal component transformation the result is a new set of uncorrelated variables. In a macroevolutionary context, therefore, a significant correlation between the average PC scores of each species in the PC space defined by the eigenvectors of **W**-matrix is an indication of coselection between both traits (in this case PCs). The reason for this is that the **B**-matrix expected under diversifying directional selection is:

$$\mathbf{B} = \mathbf{GCG}. \quad (3)$$

Where **C** is the V/CV matrix among selection gradients for the traits, in which the off-diagonal elements represent covariance between traits produced by selection (Felsenstein 1988; Zeng 1988). For example, desert environments may favor rodents with lighter fur and smaller body size. Therefore, when a species occupy this environment both traits might be coselected (selective covariance), regardless of the genetic correlation between those traits. In this way, there are two potential sources of correlated evolution among traits: common inheritance (captured in **G**, or as discussed previously, **W** in this case) and selective covariance (captured in **C**). Because PCs are uncorrelated, **G** is then a diagonal matrix in this case, and any correlation in **B** must arise from **C** (Felsenstein 1988). We are assuming here that natural selection is independent of the population phenotype. This assumption is appropriate in a macroevolutionary context where the phylogenetic branches are long enough for the peak movement to dominate the process. In this way, the main factor affecting populations' mean change is the covariance between peak movements (Felsenstein 1988).

To perform this test, each species mean was projected onto **W**'s PCs (redefined at each node) and its scores were calculated. After this, we computed the Pearson correlation between those PC scores. As a general rule, the number of PCs used in the comparisons was equal to n-1 (with the maximum of 10 PCs), with n equal the number of species being compared. We rejected the null hypothesis of evolution through drift whenever significant correlations (after Bonferroni correction) were found among at least one pair of PCs.

Both regression and correlation tests can be viewed as complementary in investigating hypotheses of phenotypic diversification. While the regression test evaluates whether variation within and between groups is proportional (deviations from proportionality indicate selection), the correlation test detects coselection (uncorrelated traits being selected together). Both tests are implemented in the R package EvolQG version 0.2–2 (Melo et al. 2015).

DIRECTIONS OF DIVERGENCE AND SELECTION QUANTIFICATION

We also explored graphically how the divergence observed among species was distributed along axes of high or low variation of the **W**-matrix (i.e., in which morphospace direction divergence among species was concentrated). Therefore, we projected the divergence observed in **B** in the same space of **W**.

We also reconstructed the potential selection gradients responsible for the morphological changes of each species. In this way, we could assess how directional selection was distributed on the phylogeny. This is a different question than simply estimating the total amount of morphological change, in the sense that here we are estimating the magnitude of selection itself, after removing the effects of patterns of covariance in the evolutionary trajectory observed. The selection gradients were reconstructed based on Lande's (1979) multivariate equation;

$$ß = \mathbf{G^{-1}}\Delta z. \quad (4)$$

Where Δz is the vector of evolutionary response, $\mathbf{G}^{-1}$ is the inverse of the genetic matrix, in this case substituted by $\mathbf{W}^{-1}$, and ß is the selection gradient vector. Matrices are always estimated with some degree of error, whether due to sampling or measurement errors, and this error is amplified whenever a matrix inversion is required. To control this noise, we calculated inverted **W**-matrices using an extension approach (described in Marroig et al. 2012). We reconstructed the ancestral states of the 38 traits using two different methods, a Brownian motion-based maximum likelihood estimator (Schluter et al. 1997) using function ace in the ape package version 3.4 in R (Paradis et al. 2004; R Core Team 2014) and linear parsimony using Mesquite version 3.02 (Maddison and Maddison 2006, 2015). We used the linear parsimony method to assess the effect of branch length in the estimation of ancestral states. After reconstructing the ancestral states, we could then calculate the vector of response to selection (Δz) as the difference vector between two nodes or between an extant species and its ancestor. We mean-standardized **W** and Δz estimates to obtain selection gradient values that were comparable among different nodes and species (Hereford et al. 2004; Hansen and Houle 2008). The strength of selection was calculated as the norm of the mean standardized ß-vector.

CLIMATIC VARIABLES

We extracted climate data for the last 30 years from each species locality georeference coordinates from the PRISM database (PRISM Climate Group 2004). For four species (*T. obscurus*, *T. cinereicollis*, *T. ruficaudus*, and *T. striatus*), however, coordinate locality data from the morphological data were unavailable; for these, we estimated climate data from random points drawn from their mapped ranges (distribution maps available from the *IUCN*, IUCN 2014). We used Worldclim climate data (Hijmans et al. 2005) for the Mexican species, *T. durangae*, since the PRISM dataset does not extend to that country. We used extreme estimates of temperature and precipitation (minimum temperature in the coldest month; maximum temperature in the warmest month measured in Celsius degrees; precipitation of wettest and driest months measured in mm) along with mean annual temperature and total precipitation indexes. We extracted that information from the climatic database using function *biovars* in package *dismo* version 1.1–1 for R (Hijmans et al. 2016). Subsequently, we estimated the impact of the climatic variables on the morphological variation through an evolutionary regression implemented in SLOUCH package version 1.0 for R (Hansen et al. 2008). The idea behind this analysis is to disentangle effects of phylogenetic inertia, the evolutionary lag between a species' traits and its optimum values, from effects of adapting to an optimum that is influenced by the predictor variable. The model is built around an Ornstein–Uhlenbeck model (OU) of adaptive evolution for a single trait, while the predictor variable is modeled as a Brownian Motion (BM) process (Hansen et al. 2008). The method uses generalized least squares to estimate the regression parameters, i.e. the influence of the predictor variable on the primary optimum. It also uses maximum likelihood to jointly estimate phylogenetic inertia (represented by a parameter called phylogenetic half-life, $t_{1/2}$) and stochasticity (v_y) effects. Those stochastic effects can be interpreted as unmeasured selective forces and/or drift effects (Voje and Hansen 2013). By disentangling phylogenetic effects due to phylogenetic inertia (slowness of adaptation) from those due to closely related species adapting to similar environments, this test is a better choice when trying to estimate the impact of a certain variable in the evolution of a group (Hansen et al. 2008). The analysis, thus, returns an estimate of the regression coefficient of the linear regression, taking into account the phylogenetic history of a clade.

We used these climatic variables as predictor variables, and the scores of each species for the first two PCs of **W** as the response variables. Measurement error, in both predictor and response variables, might impact the estimation of the evolutionary regression. To accommodate this potential uncertainty, we included the variance of each individual parameter in the analyses (Hansen and Bartoszek 2012). We compared the relative support for each model in relation to models estimated without the

predictor variable using Akaike's Information Criterion correction for small sample sizes, AICc. A model was considered the best fit for the data if its AICc value was at least two units lower than the model without predictor (Hansen et al. 2008). High values of the coefficient of determination r^2 indicate that a high amount of morphological variation is explained by the predictor variable. Because the estimation of phylogenetic inertia ($t_{1/2}$) is rather inaccurate in small phylogenies (<30 terminals), we focused our comparisons in the outcome of the evolutionary regression and estimated the regression in two different scenarios as suggested by Hansen et al. (2008). In the first, we explored the likelihood surface in scenarios with small phylogenetic effect, with $t^1/_2$ ranging from 0 to 0.1 (10% of the total length of the tree scaled to unit length). In the second, we allowed high values of phylogenetic inertia, from 0 to 100% of the total length of the tree.

Lastly, we investigated the relationship between magnitude of selection and the magnitude of change in climatic niches using a linear regression. We reconstructed climatic niche using a Brownian motion process and estimated magnitude of climatic niche change as the norm of the difference vector between reconstructed climatic values from derived to ancestral nodes. Then we correlated the magnitude of climatic niche change with the magnitude of selection reconstructed using maximum likelihood, squared parsimony, and linear parsimony (see Supplementary Material for details).

All analyses were performed in the free available software R version 3.2.1 (R Core Team 2014), using the above cited libraries and functions. Codes used are available on Github/paulaassis/Macroevolution and data are available as supplementary files.

Results

GENETIC DRIFT TESTS

Both regression and correlation approaches indicate that morphological evolution in *Neotamias* cannot be explained by genetic drift alone, thus supporting natural selection as the most probable evolutionary process responsible for *Neotamias* cranial morphology diversification (Fig. 2). In the regression test, of the 12 hierarchical levels analyzed, four have slopes significantly different from one: node 1 (all *Neotamias* + *T. striatus*), node 2, node 3, and node 10 (small-bodied *Neotamias*) (Fig. 2 and Fig. S4, Table 1). Divergence within these groups is therefore unlikely to be due to genetic drift alone.

For the correlation test, significant correlations were found for nodes 1 (all *Neotamias* + *T. striatus*), 2, 3, 4, 7 (*quadrivittatus* group), 8, and 11 (*townsendii* or large-bodied group), indicating deviations from the expectation under genetic drift in each case (Fig. 2, Table 1). In most comparisons, PC1 was significantly correlated with the remaining PCs, except for node 11 (*townsendii* or large-bodied group), where the only correlation observed was between PC3 and PC5. Considering results of both drift tests together, genetic drift was rejected as an explanation for the three more inclusive nodes in phylogeny (node 1, 2, and 3; Fig. 2, Table 1). As one moves further along the phylogeny, shallower branches show a less clear picture with genetic drift being rejected for at least one test for the majority of nodes. In only four, out of 12 nodes, phenotypic diversification was consistent with the null hypothesis of genetic drift (nodes 5, 6, 9, and 12).

DIRECTIONS OF DIVERGENCE AND SELECTION QUANTIFICATION

Most of the divergence observed between *Neotamias* species was along the first principal component of **W**. For some nodes, ~80% of the total divergence among species occurred along PC1 (nodes 1, 2, 3, 6, and 10; Fig. 3). PC1 is an allometric vector representing variation in cranial size and associated shape, with most loadings pointing in the same direction (Table S6, Fig. 4). Moreover, species means projection on PC1 is highly correlated with centroid size corroborating that it is a good estimate of size (r^2 = 0 .99, Table S7). Therefore, most of the divergence in this group can be attributed to size-related change. The only group that deviates from this pattern are species in the southern Rocky Mountains (as defined by Reid 2012; including *T. umbrinus*, *T. rufus*, *T. quadrivittatus*, *T. cinereicollis*, *T. dorsalis*, *T. canipes*). In this group, PCs 3 and 4 both had higher percentages of divergence than expected by drift, while PC1 divergence was in accordance with a drift scenario.

The magnitude of selection varied greatly among branches and the models used to reconstruct (linear parsimony and maximum likelihood). In general, smaller estimates are concentrated on more basal nodes, indicating that selection was stronger in the more recent branches (Fig. 5). Moreover, even though both methods showed large differences in the estimates for the small-bodied chipmunks clade (*T. alpinus*, *T. amoenus, T. ruficaudus*, and *T. minimus*), the group leading to the species *T. alpinus* and *T. minimus* presented the highest estimates of selection (Fig. 5), indicating that in this particular clade selection was very strong.

PHENOTYPE–ENVIRONMENT CORRELATION

We found several high correlations between the first two PCs and climatic variables. The first two PCs of the pooled-within-species variance/covariance (V/CV) matrix are displayed in Table S6 and Figure 4, with the 38 cranial traits classified according to functional/developmental groups. Together, these PCs account for 42.2% of the total within-species variation. PC1, as mentioned, is an allometric size vector, while PC2 is mainly a contrast between traits that affected the length of the face and the width of the neurocranium (Fig. 4). In the context of the functional/developmental groups, PC2 contrasts larger oral/nasal group distances with

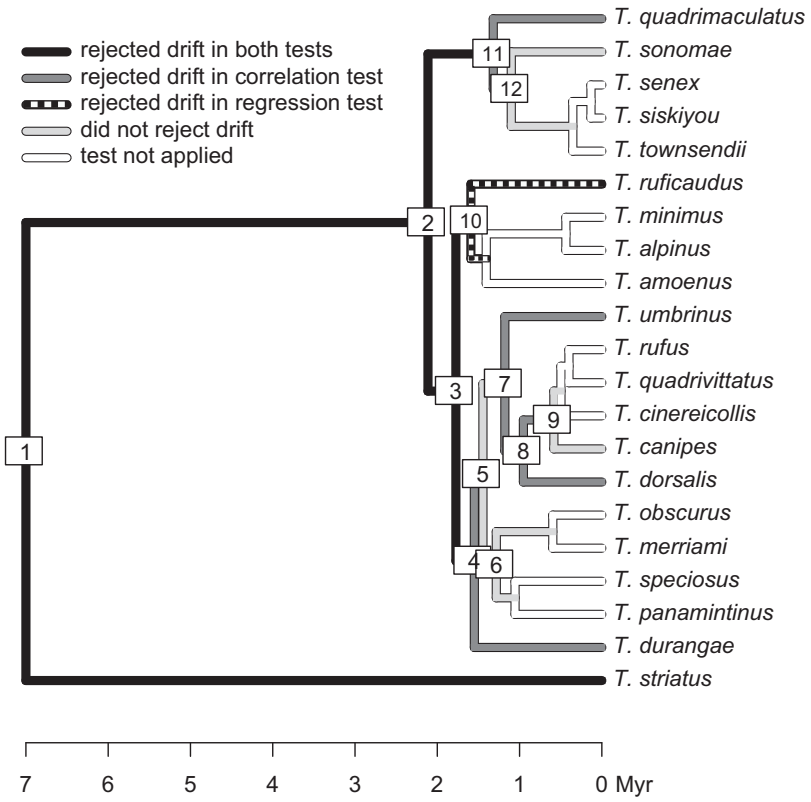

Figure 2. Phylogeny displaying the results of the genetic drift tests. The values close to the nodes represent the node number referred in the Table 1 and Figure S4. No tests were performed for nodes with three or fewer species. The scale bar represents time in million of years. Phylogeny based on four nuclear genes from Reid et al. (2012) and Sullivan et al. (2014).

Table 1. Genetic drift test results, showing the slope (b) of the regression line calculated between W-matrix and B-matrix for the regression test with confidence interval.

	Regression test			Correlation test	
		95% CI			
Node label	b	Lower	Upper	PCs included	Correlated PCs
1	**1.215**	**1.082**	**1.349**	10	1-(2,4,9); 4-(9)
2	**1.204**	**1.071**	**1.337**	10	1-(2,4,9);2-(9); 4-(9)
3	**1.166**	**1.007**	**1.325**	10	1-(4,8)
4	1.094	0.961	1.226	10	1-(8)
5	1.072	0.936	1.209	9	–
6	0.979	0.733	1.225	3	–
7	1.017	0.846	1.189	5	1-(5)
8	1.008	0.808	1.207	4	1- (3)
9	0.975	0.769	1.182	3	–
10	**1.328**	**1.051**	**1.606**	3	–
11	1.012	0.838	1.186	4	3-(4)
12	0.958	0.753	1.162	3	–

Regression coefficients significantly different from 1.0 are shown in bold. The node labels correspond to the node number displayed in Figure 2. For each node all species in the node were included in the drift tests. For the correlation test we present the number of PCs included (n-1 of the number of species with a maximum of 10) and the PCs where we found any correlation. The first number corresponds to a specific PC and the numbers in parentheses are the PCs to which a significant correlation was found.

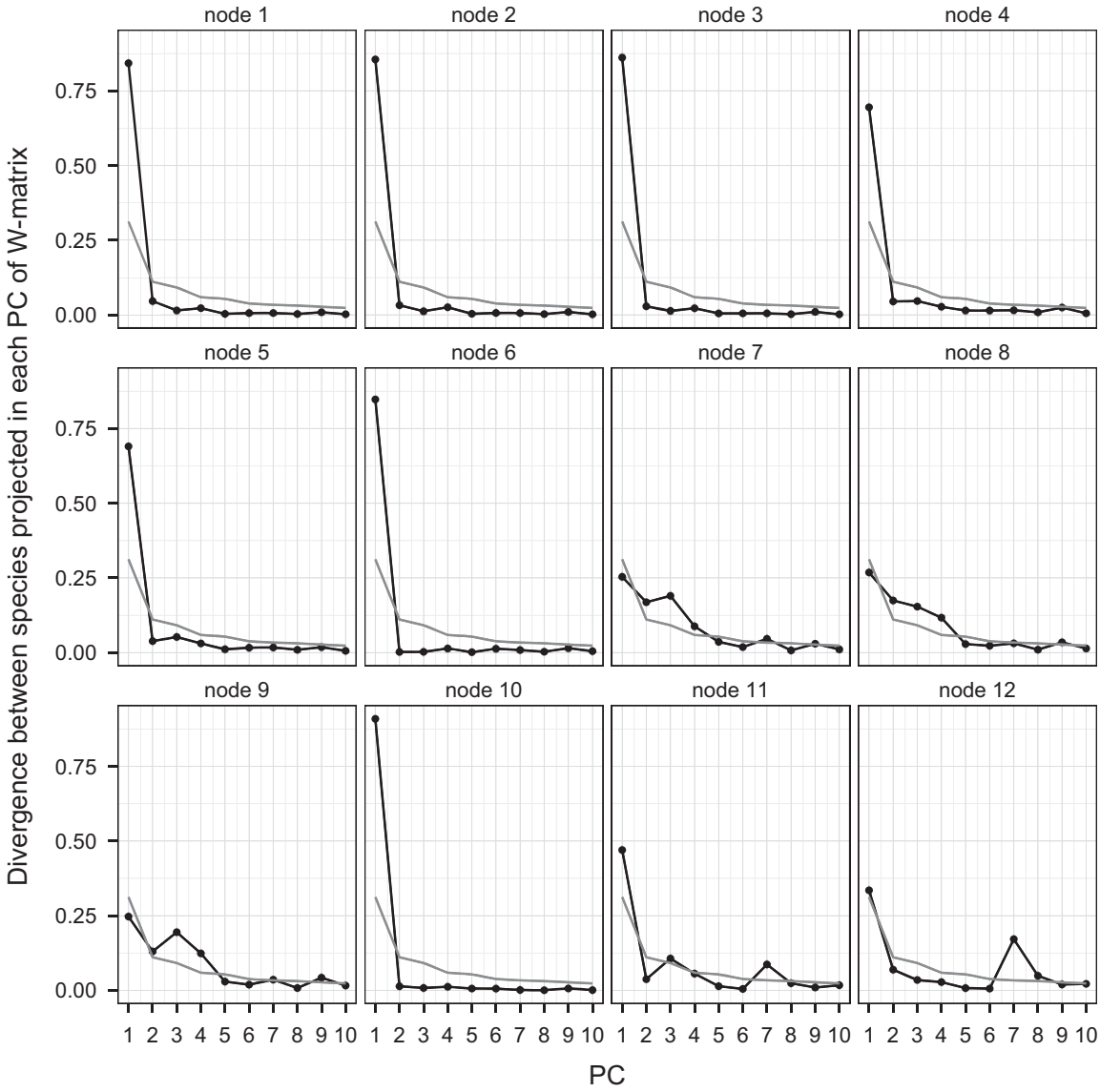

Figure 3. Directions of divergence between species (B) projected into the first 10 principal components of the W-matrix (black lines and points). Gray lines represent the percentage of variance explained by each principal component of the ancestral W-matrix (Table S6). For the majority of nodes most divergence between species occurred along PC1, in some cases it represented more than 70% of the total divergence among species (nodes 1, 2, 3, 4, 5, 6, and 10).

smaller zygomatic ones, suggesting a narrowing of the zygomatic arch. The second PC also represents a factor where an enlarged frontal bone contrasts with a smaller cranial vault (Table S6).

For the comparisons involving PC1, minimum temperature of the coldest month and mean annual temperature were the only climatic variables that had a better predictive power than the model without predictor (AICc values more than 2 units smaller). Minimum temperature of the coldest month explained from 39.9 to 48.7% of the total variance in the scenario of strong and mild phylogenetic inertia, respectively (Table 2). For the annual mean temperature, the total amount of variance explained was smaller, ranging from 24.5 to 34.2 % (Table 2, strong and mild phylogenetic inertia). Since PC1 is an allometric size vector, these results suggest that smaller animals live in relatively colder environments (Fig. 6).

For PC2, all climatic variables analyzed had a better predictive power than the model without predictor (lower AICc values). However, maximum temperature of the warmest month and precipitation of the driest month explained very little of the morphological variation (1.10–3.26 % and 10.53–6.14% strong and mild phylogenetic inertia, respectively). Annual mean temperature, minimum temperature of the coldest month, annual precipitation, and precipitation of wettest month explained a high amount of the morphological variation ranging from 22 to 45% (Table 2).

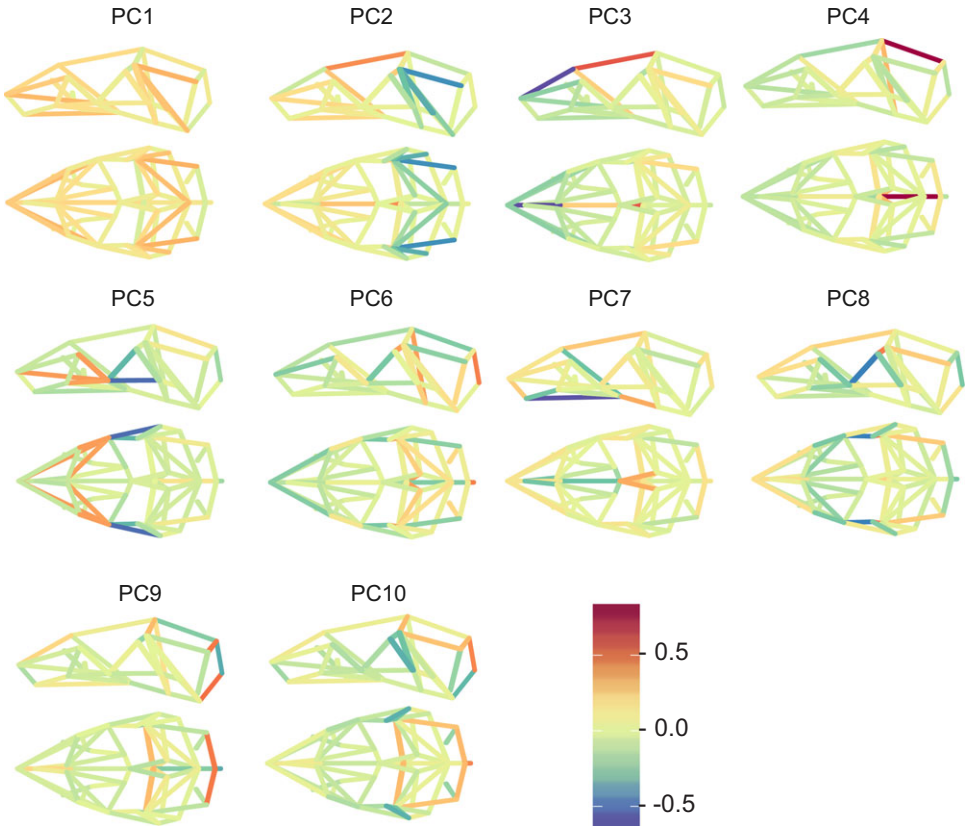

Figure 4. Schematic representation of the *Neotamias* ancestral W-matrix principal components loadings for each trait. The first row corresponds to a skull's lateral view and second row to ventral view. Distances represented can be identified in Figure 1 and loadings in Table S6. The color scheme represents the loadings estimated for each PC.

Since PC2 is a contrast between face length and neurocranium width, this result indicates that species with shorter faces in relation to a wider neurocranium (lower PC2 scores) tend to live in colder and dryer areas (Fig. 6).

The regression between climatic niche reconstruction and selection strength showed inconclusive results, with the reconstruction method greatly affecting the regression results (Fig. S5). For ancestral states reconstructed with maximum likelihood and squared parsimony there is an indication that the higher the selection strength the higher the climatic niche change. On the other hand, for reconstruction using linear parsimony no correlation was observed.

Discussion

Neotamias chipmunks represent one of the most speciose clades of North American mammals, exhibiting the hallmarks of a recent and rapid radiation, one that contrasts sharply with its sister group that apparently has not undergone any speciation event (Good et al. 2003; Reid et al. 2012; Sullivan et al. 2014). Here, we provide evidence supporting the long-held hypothesis that morphological variation in the group cannot be explained solely by genetic drift but rather evolved in association with the ecological niches occupied (Allen 1890; Patterson 1980, 1983; Sutton and Patterson 2000). To this end, we used an integrative framework that combines phylogenetic comparative methods with quantitative genetics to provide a comprehensive means to examine the association between evolutionary processes and potential selective agents during species diversification.

The overall pattern for the 20 species in the *Neotamias* clade is one of too much variation between populations for divergence to have occurred solely by genetic drift. Eight of the 12 phylogenetic groups where tests could be applied rejected drift by one or both of the tests we applied; three of the four nodes that did not reject drift had only four descendent species. Since the power of both tests is dependent upon sample size in each comparison, that power diminishes substantially when too few species are included (Marroig and Cheverud 2004; Harmon and Gibson 2006). It is likely that sample size in these three tests influenced the results. That natural selection has shaped the phenotypic evolution of these species is not surprising, since most biologists agree that natural selection is important at the morphological level. On the other hand, the mere existence of a speciose lineage does not

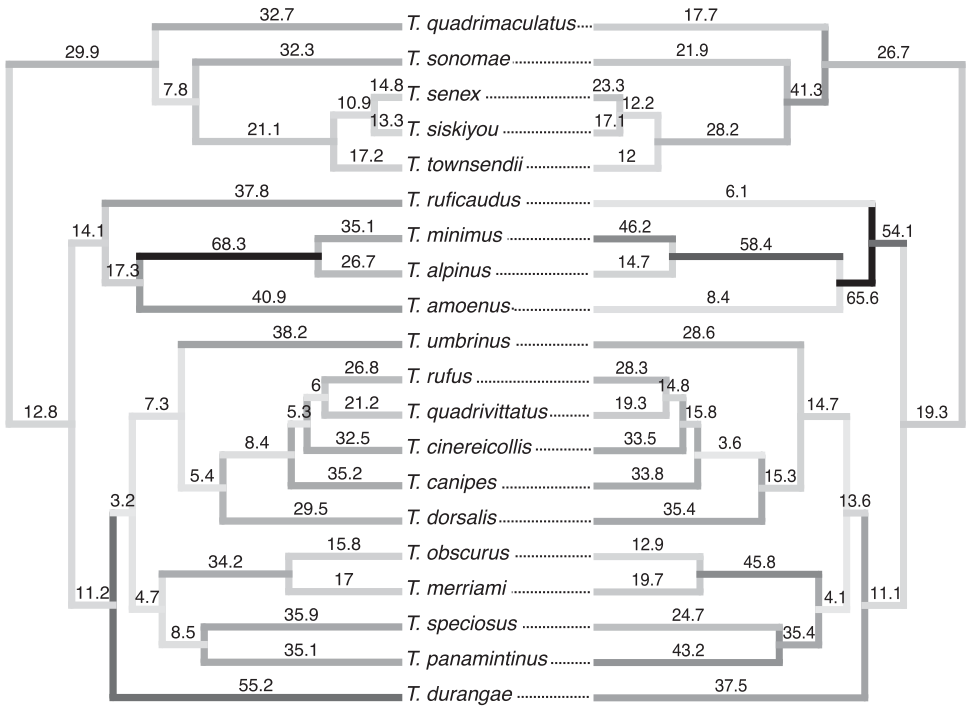

Figure 5. **(A) Phylogeny displaying the strength of selection estimates: on the left are values obtained using a maximum likelihood ancestral state reconstruction, on the right are selection strength values reconstructed using linear parsimony. Colors represent the magnitude of selection (absolute value above branch) with increasing values going from gray to black. The estimated r^2 between the different reconstructions methods is equal to 0.43 and $P < 0.001$.**

necessarily imply that member taxa have diversified solely or mainly by adaptive means (Schluter 2000).

Most of the divergence observed among species was along the first principal component, which at first glance might suggest that genetic constraints dominated the diversification in this group. In this multivariate context, genetic constraints can be understood as the impact of the axis of greatest variation (PC1) on the evolutionary change. In other words, simply because there is more variation in the direction of PC1, the response to selection could be biased along PC1, even if selection was acting in another direction. The hypothesis that patterns of variation might constrain and bias evolutionary change was first proposed by Schluter (1996), who emphasized that this bias should be more marked during rapid radiations, as is *Neotamias* (Sullivan et al. 2014). Alternatively, divergence along PC1 could be the result of selection in the direction of PC1. We will deal with disentangling the relative contributions of genetic constraints and selection in those observed patterns of divergence in a future contribution.

The correlations observed between morphological traits and several climatic variables (PC1 × minimum temperature of coldest month and annual mean temperature; PC2 × minimum temperature of coldest month, annual mean temperature, annual precipitation, and precipitation of wettest month) suggest that some morphological differences among species likely reflect the climatic differences among the habitats they occupy. Even though we were unable to access the relative role of phylogenetic inertia (because of the limited number of species in the phylogeny), the amount of variance explained by the predictor variables remained similar under both low and high degrees of phylogenetic inertia, indicating that the regression coefficient estimates were robust. Considering the temperature variables, minimum temperature of the coldest month had both the higher regression coefficients for both PC1 and PC2 and a better model fit (smaller AICc-Table 2, Fig. 6). This indicates that minimum temperatures had a greater impact on the expressed morphological variation than higher temperatures or mean annual temperature. These correlations also suggest that species with higher scores on these two PC axes inhabit places with higher temperatures and species with lower scores occur in colder habitats (Fig. 6). Considering that the first morphological PC is an allometric size component, this is exactly the opposite of what would be expected according to Bergmann's Rule, the ecogeographic prediction that organisms living in colder climates should have larger body sizes and, alternatively, that warm-climate denizens should have smaller body sizes (Bergmann 1847; Mayr 1970). This positive correlation is not surprising since the smaller chipmunks are those that inhabit the highest elevations (*T. minimus scrutator* and *T. alpinus*, e.g., both of which extend into the arctic-alpine zone above 10,000

Table 2. Phylogenetic evolutionary regressions for effects of climatic variables on morphological PCs scores.

Response variable		**Model type 1**: Strong phylogenetic inertia			**Model type 2**: Mild phylogenetic inertia		
	Predictor variable	r^2 (%var)	AICc	Slope ± SE	r^2 (%var)	AICc	Slope ± SE
PC1	Annual mean temperature (°C)	24.59	**101.57**	0.047 ± 0.018	34.24	**110.75**	0.068 ± 0.021
PC1	Max temperature of Warmest month (°C)	0.89	106.64	0.008 ± 0.19	7.43	117.70	0.033 ± 0.026
PC1	Min temperature of Coldest month (°C)	39.94	**97.69**	0.046 ± 0.012	48.97	**105.60**	0.061 ± 0.014
PC1	Annual precipitation (mm^3)	16.07	103.72	0.003 ± 0.002	16.74	115.56	0.004 ± 0.002
PC1	Precipitation of wettest month (mm^3)	18.59	103.20	0.018 ± 0.008	18.51	115.13	0.021 ± 0.010
PC1	Precipitation of driest month (mm^3)	0.04	106.79	−0.006 ± 0.064	0.42	119.19	−0.025 ± 0.087
PC1	–	–	103.63		–	116.11	
PC2	Annual mean temperature (°C)	29.45	**46.26**	0.013 ± 0.005	30.67	**49.98**	0.014 ± 0.005
PC2	Max temperature of warmest month (°C)	1.10	51.51	0.002 ± 0.005	3.26	56.11	0.005 ± 0.006
PC2	Min temperature of coldest month (°C)	41.54	**44.30**	0.012 ± 0.003	43.54	**46.26**	0.012 ± 0.003
PC2	Annual precipitation (mm^3)	17.35	48.90	0.001 ± 0.000	21.73	52.15	0.001 ± 0.000
PC2	Precipitation of wettest month (mm^3)	25.20	**47.58**	0.005 ± 0.002	26.93	**50.88**	0.005 ± 0.002
PC2	Precipitation of driest month (mm^3)	10.53	49.96	−0.023 ± 0.018	6.14	55.51	−0.020 ± 0.019
PC2	–	–	101.95	–	–	113.04	–

The analyses were performed in two different scenarios: model type 1 where strong phylogenetic inertia was explored ($t^1/_2$ values ranging from 0–total length of the tree) and model type 2 where a mild phylogenetic inertia was allowed ($t^1/_2$ values ranging from 0–10% of total tree length). The values correspond to the best estimate model-fit in a given scenario. Lower values of AICc indicate models with best fit compared to the model with no predictor variable (Brownian motion). The amount of variance explained by the predictor variable in each model (r^2), evolutionary regression slope, and standard error are also shown.

ft) and, therefore, endure the lowest temperatures. Interestingly, the branch leading to these two species was also the one where we observed the strongest selection strength, which also supports the hypothesis that minimum temperature (or other environmental aspect correlated with minimum temperature) has been an important selective agent. At the other extreme, species of the *townsendii* group (*T. townsendii*, *T. senex*, *T. siskiyou*, *T. quadrimaculatus*, *T. sonomae*) are the largest chipmunks and occupy mostly coastal areas at lower elevations and with seasonally more moderate climate. One possible explanation for this trend is that species living in warmer climates experience longer growing seasons and shorter hibernation periods, attributes that may lead to greater growth potential and thus to larger body size, which has already been demonstrated for other hibernating mammals (Ozgul et al. 2010; Eastman et al. 2012).

In a similar fashion, species with higher loadings on the second PC axis, those with longer faces and narrower neurocrania, inhabit hotter climates while those with lower scores (wider neurocrania and shorter faces) occur in colder environments. This pattern conforms to what we would expect according to Allen's rule, which predicts that animals living in colder environment should have relatively shorter and stouter extremities (such as the snout) to reduce heat loss (Allen 1877; Yom-Tov and Nix 1986). One of the species with small loadings in both PC1 and PC2, the least chipmunk (*T. minimus*), occupies the widest distribution of all western chipmunks (Reid 2006), and therefore occurs in places with very different temperature indices. Our analyses, however, are exclusive to the subspecies *T. minimus scrutator*, which is confined to sagebrush steppe in the Great Basin and eastern slope of the Sierra Nevada, extending above treeline in some parts of that high range (Johnson 1943; Reid 2006). Thus, a more broad-based geographic sampling of *T. minimus* would represent an opportunity to assess if the interspecific patterns of morphological and climatic relationship observed have correspondence at the intraspecific level. If so, this would reinforce the important role of environmental variables in determining morphological variation.

Precipitation has been hypothesized to be equally important to temperature as the mechanistic basis for body size trends observed in mammals (Burnett 1983; Millien et al. 2006). The rationality behind this hypothesis is that wetter habitats will have higher primary productivity, and consequently greater food availability, which could lead to bigger animals (Burnett 1983). However, in our analyses precipitation variables explained a low amount of the morphological PC1 (allometric size; Table 2), and the associated AICc values were similar to the model without a predictor. Those results contravene Burnett's hypothesis of precipitation as an evolutionary driver of body size diversification, at least in these chipmunks. On the other hand, the evolutionary regressions between PC2 and both precipitation of the wettest month as well as annual precipitation had smaller

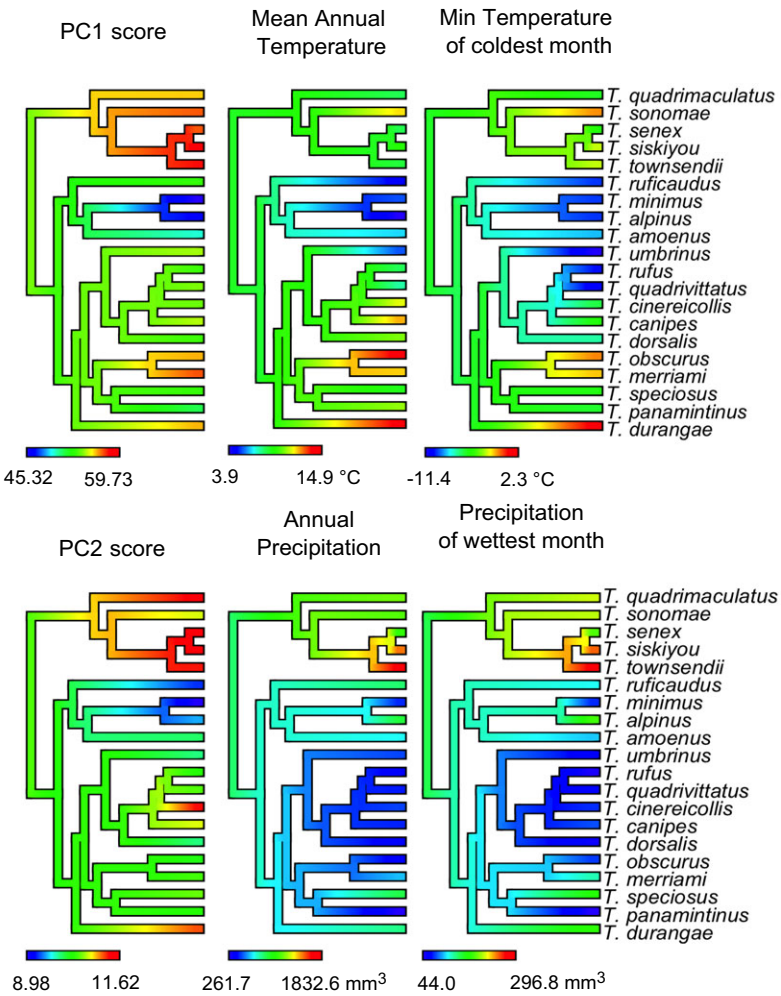

Figure 6. **Schematic plots of the observed mean values for morphological (PC1, PC2 score) and climatic variables (the ones with greater explaining power in Table 2). The scale bars under each phylogeny indicate the observed values in the scores of the morphological PCs or the respective temperature or precipitation index.**

AICc values compared to the model without predictor, explaining about 20% of the morphological variation in PC2 (Table 2). These relations mean that species with shorter faces and wider neurocrania inhabit dryer habitats and those with longer faces and narrower neurocrania occur in wetter places (Fig. 6). Species of the *townsendii* group, with higher loadings in PC2 living in the wettest environments, once again are on one extreme of this trend, while those living in dry-habitats have smaller PC2 scores (Fig. 6). Ball and Roth (1995) argued that the presence of cheek pouches in chipmunks affects the relative size of the snout, creating a larger diastema between incisors and posterior tooth row. Therefore, species with relative longer snout might have bigger cheek pouches, which would be advantageous in a high productivity environment (wetter environments).

Felsenstein (1988) defined "selective covariance is the covariance in the distribution of traits, owing to covariance of the changes in these traits brought about by a correlation of their selection pressures." Therefore, a more holistic picture of these chipmunks' skull evolution can be gained by considering all analysis together. The selective covariance recovered between PC1 and PC2 (Table 1), the results from the evolutionary regression and the estimates of selection strength point to a scenario where minimum temperature of the coldest month has been the most important agent in cranial diversification and a potential source for the selective covariance. Thus, the lower the temperature the higher the selective force on morphological attributes. A possible functional explanation for this trend is that species in colder climates experience shorter growing seasons, leading to smaller animals (PC1). Simultaneously, colder environments may have selected for stouter extremities to prevent heat loss, which in turn may have led to the positive correlation observed between PC1 and PC2 between species, as discussed above. An interesting follow-up to our work would be to examine the degree of convolution, which would measure the area of the nasomucosal

membrane system, of the turbinate bones in species at the opposite end of the PC2 spectrum. Given that these membranes are responsible, in large part, for controlling heat and water loss in mammals (Schmidt-Nielsen et al. 1970; Van Valkenburgh et al. 2004).

It is important to keep in mind that we used **P**-matrices as a substitute for the genetic counterpart in all analyses performed. By definition, **P**-matrices occupy a larger volume than that of their underlying **G**-matrices (due to the addition of the environmental effects; Falconer and Mackay 1996). Therefore, the selection strengths reconstructed here cannot be directly compared to estimates derived from **G**-matrix studies. Thus, we used the **P**-matrix only in a comparative way, to inform us where selection was strongest inside the phylogenetic history of western chipmunks. Moreover, even though we found a high degree of similarity among **P**-matrices, comparisons involving *T. durangae* showed moderate dissimilarity between matrices (lowest comparison 0.64, Table S3 and S4). This is the species with the lowest sample size, which could be the reason for such low values of matrix comparisons. Moreover, covariance matrices estimated with small sample sizes cause an upward bias for the leading eigenvalues (Marroig et al. 2012). In our study, the regression between eigenvalues coefficient of variation and sample size was marginally significant ($r^2 = 0.14$, $P = 0.052$, Fig. S2 and S3). This indicates that particularly for *T. durangae*, this might influence the results drawn from this taxon, especially for the reconstructed selection gradient in the branch leading to this species. Therefore, we advise caution when interpreting any result regarding this particular species. Sample size unbalance does not appear to be affecting the estimation of the ancestral **W**-matrices (Table S5).

The distribution of some of these chipmunk species has changed in the last century due to climate change (Moritz et al. 2008): some have shifted their elevational distribution (e.g., *T. alpinus*), others their latitudinal distribution (e.g., *T. senex*). In the Sierra Nevada of California, which encompasses the range of nine chipmunk species, including both *T. alpinus* and *T. senex*, minimum temperature of the coldest month has increased over the past century while maximum temperature of the warmest month has remained constant (Rowe et al. 2015). We showed that minimum temperature is one of the most important climatic variables associated with morphological attributes of chipmunks. Hence, we might expect that climatic change would affect not only their distribution, but also their morphology. Consequently, we might predict that species living in colder areas will be most affected by those changes, and might respond by becoming morphologically more similar to their warm climate cousins. In fact, one study analyzing two of those chipmunk species (*T. alpinus* and *T. speciosus*) found that in the last 100 years *T. alpinus* (which lives in colder environments) is indeed responding to climate change more pronouncedly than *T. speciosus*. This study also showed that this species has actually changed its diet, suggesting another mechanism by which climate might influence morphological variation in these species, that is by changing food resources (Walsh et al. 2016).

Although we cannot pinpoint the mechanistic factors that led to the correlations observed, the association between climatic variables and cranial morphology suggests that abiotic environmental conditions are remarkably important in determining skull morphology in *Tamias*, either directly through influences on the growth period or indirectly via food availability (Patterson 1980, 1983; Sutton and Patterson 2000). We only tested a few a priori hypotheses of the abiotic niche dimensions of these species thought to be important for the group (Allen 1890; Patterson 1980, 1983; Sutton and Patterson 2000). Thus, it is likely that unmeasured ecological variables are equally important determinants of morphological variation as are those climatic variables we examined. A study measuring exactly the availability of food in the habitats of each species would be an interesting follow-up to our work and a very informative way to specifically test the importance of both temperature and precipitation variables. Another important venue of future research would be to investigate the biophysical functional significance of the traits we examined structurally.

ACKNOWLEDGMENTS

We thank the Museum of Vertebrate Zoology and National Museum of Natural History curators for making specimens available for our use. Specimens for several of the species examined were collected under the auspices of the California Department of Fish and Wildlife. We thank J. Sullivan and J. Demboski for providing the dated phylogenetic tree; B.M.A. Costa for providing valuable help in establishing the landmarks and distances in chipmunks; M. Zelditch for intellectual input throughout the development of this work; C. Patton, L. Chow, P. Moore, G. Lefèvre for field assistance; G. Garcia for help with the figures; A. Penna, M. N. Simon, A. Porto, P. Guimarães Jr, I. Dworkin, and two anonymous reviewers for helpful comments on previous versions of the manuscript. This work was supported by funds from a PhD scholarship granted to A.P.A.A. from the Fundação de Amparo à Pesquisa do Estado de São Paulo - FAPESP, grants # 2010/52369-0 and 2012/00852-4. G.M. and D.M.R. were also supported by FAPESP grants (2011/14295-7 and 2014/12632-4). The authors have no conflict of interest to declare.

DATA ARCHIVING

The doi for our data is 10.5061/dryad.3583j.

LITERATURE CITED

Ackermann, R. R., and J. M. Cheverud. 2002. Discerning evolutionary processes in patterns of tamarin (genus Saguinus) craniofacial variation. Am. J. Phys. Anthropol. 117:260–71.

———. 2004. Detecting genetic drift versus selection in human evolution. Proc. Natl. Acad. Sci. USA 101:17946–17951.

Adams, D. C., F. J. Rohlf, and D. E. Slice. 2013. A field comes of age: geometric morphometrics in the 21st century. Hystrix 24:7.

Allen, J. A. 1877. The influence of physical conditions in the genesis of species. Radic. Rev. 1:108–140.

———. 1890. A review of some of the North American ground squirrels of the genus Tamias. Bull. Am. Mus. Nat. Hist. 3:45–116.

Ball, S. S., and V. L. Roth. 1995. Jaw muscles of new world squirrels. J. Morphol. 224:265–291.

Barnosky, A. D., E. A. Hadly, and C. J. Bell. 2003. Mammalian response to global warming on varied temporal scales. J. Mammal. 84:354–368.

Bergmann, K. G. L. C. 1847. Über die Verhältnisse der wärmeokönomie der Thiere zu ihrer Grösse. Gött. Stud. 3:595–708.

Bergstrom, B. J. 1992. Parapatry and encounter competition between chipmunk (Tamias) species and the hypothesized role of parasitism. Am. Midl. Nat. 128:168–179.

Blows, M. W., S. F. Chenoweth, and E. Hine. 2004. Orientation of the genetic variance-covariance matrix and the fitness surface for multiple male sexually selected traits. Am. Nat. 163:329–340.

Burnett, C. D. 1983. Geographic and climatic correlates of morphological variation in *Eptesicus fuscus*. J. Mammal. 64:437.

Cheverud, J. M. 1982. Phenotypic, genetic, and environmental morphological integration in the cranium. Evolution 36:499–516.

———. 1988. A comparison of genetic and phenotypic correlations. Evolution 42:958–968.

Cheverud, J. M., and G. Marroig. 2007. Comparing covariance matrices: random skewers method compared to the common principal components model. Genet. Mol. Biol. 30:461–469.

Cox, P. G., E. J. Rayfield, M. J. Fagan, A. Herrel, T. C. Pataky, and N. Jeffery. 2012. Functional evolution of the feeding system in rodents. PLoS ONE 7:e36299.

Eastman, L. M., T. L. Morelli, K. C. Rowe, C. J. Conroy, and C. Moritz. 2012. Size increase in high elevation ground squirrels over the last century. Glob. Change Biol. 18:1499–1508.

Elbroch, M. 2006. Animal skulls: a guide to North American species. Stackpole Books, Mechanicsburg, Pennsylvania, 727 pp.

Falconer, D. S., and T. F. C. Mackay. 1996. Introduction to quantitative genetics. 4th ed. Addison Wesley Longman, Harlow, Essex.

Felsenstein, J. 1988. Phylogenies and quantitative characters. Annu. Rev. Ecol. Syst. 19:445–471.

Good, J. M., J. R. Demboski, D. W. Nagorsen, and J. Sullivan. 2003. Phylogeography and introgressive hybridization: Chipmunks (genus *Tamias*) in the Northern Rocky Mountains. Evolution 57:1900–1916.

Grinnell, J., and T. I. Storer. 1924. Animal life in the Yosemite: an account of the mammals, birds, reptiles, and amphibians in a cross-section of the Sierra Nevada. University Press, Berkeley, California.

Hansen, T. F., and K. Bartoszek. 2012. Interpreting the evolutionary regression: the interplay between observational and biological errors in phylogenetic comparative studies. Syst. Biol. 61:413–425.

Hansen, T. F., and D. Houle. 2008. Measuring and comparing evolvability and constraint in multivariate characters. J. Evol. Biol. 21:1201–1219.

Hansen, T. F., J. Pienaar, and S. H. Orzack. 2008. A comparative method for studying adaptation to a randomly evolving environment. Evolution 62:1965–1977.

Harmon, L., and R. Gibson. 2006. Multivariate phenotypic evolution among island and mainland populations of the ornate day gecko, *Phelsuma ornata*. Evolution 60:2622–2632.

Heller, H. C. 1971. Altitudinal zonation of chipmunks (*Eutamias*): interspecific aggression. Ecology 52:312–319.

Heller, H. C., and D. M. Gates. 1971. Altitudinal zonation of chipmunks (*Eutamias*): energy budgets. Ecology 52:424–433.

Heller, H. C., and T. Poulson. 1972. Altitudinal zonation of chipmunks (*Eutamias*): adaptations to aridity and high temperature. Am. Midl. Nat. 87:296–313.

Hereford, J., T. F. Hansen, and D. Houle. 2004. Comparing strengths of directional selection: how strong is strong? Evolution 58:2133.

Hijmans, R. J., S. E. Cameron, J. L. Parra, P. G. Jones, and A. Jarvis. 2005. Very high resolution interpolated climate surfaces for global land areas. Int. J. Climatol. 25:1965–1978.

Hijmans, R. J., S. Phillips, J. Leathwick, and J. Elith. 2016. dismo: species distribution modeling. R package version 1.1-1. Available at https://CRAN.R-project.org/package=dismo.

Hohenlohe, P. A., and S. J. Arnold. 2008. MIPod: a hypothesis testing framework for microevolutionary inference from patterns of divergence. Am. Nat. 171:366–385.

IPCC. 2014. Climate change 2014: impacts, adaptation, and vulnerability. contribution of working group II to the fifth assessment report of the intergovernmental panel on climate change. Cambridge Univ. Press, Cambridge, U. K. and New York, NY.

IUCN. 2014. The IUCN red list of threatened species. Version 2014.3.

Johnson, D. H. 1943. Systematic review of the chipmunks (genus *Eutamias*) of California. California Univ. Press, California.

Krzanowsky, W. J. 1979. Between-groups comparison of principal components. J. Am. Stat. Assoc. 74:703–707.

Lande, R. 1979. Quantitative genetic analysis of multivariate evolution, applied to brain: body size allometry. Evolution 33:402–416.

———. 1980. Genetic variation and phenotypic evolution during allopatric speciation. Am. Nat. 116:463–479.

Lessels, C. M., and P. T. Boag. 1987. Unrepeatable repeatabilities: a common mistake. The Auk 104:116–121.

Linde, K. van der, and D. Houle. 2009. Inferring the nature of allometry from geometric data. Evol. Biol. 36:311–322.

Lofsvold, D. 1988. Quantitative genetics of morphological differentiation in peromyscus. II. Analysis of selection and drift. Evolution 42: 54–67.

Maddison, W. P., and D. R. Maddison. 2006. StochChar: a package of Mesquite modules for stochastic models of character evolution. Available at www.mesquiteproject.org, Version 1.06.

———. 2015. Mesquite: a modular system for evolutionary analysis. Available at www.mesquiteproject.org, Version 3.02.

Marroig, G., and J. M. Cheverud. 2001. A comparison of phenotypic variation and covariation patterns and the role of phylogeny, ecology, and ontogeny during cranial evolution of new world monkeys. Evolution 55:2576–2600.

———. 2004. Did natural selection or genetic drift produce the cranial diversification of neotropical monkeys? Am. Nat. 163:417–428.

Marroig, G., D. A. R. Melo, and G. Garcia. 2012. Modularity, noise and natural selection. Evolution 66:1506–1524.

Mayr, E. 1970. Populations, species, and evolution: an abridgment of animal species and evolution. Harvard Univ. Press, Harvard.

Melo, D., G. Garcia, A. Hubbe, A. P. Assis, and G. Marroig. 2015. EvolQG—an R package for evolutionary quantitative genetics. F1000Research, doi: 10.12688/f1000research.7082.1.

Millien, V., S. Kathleen Lyons, L. Olson, F. A. Smith, A. B. Wilson, and Y. Yom-Tov. 2006. Ecotypic variation in the context of global climate change: revisiting the rules. Ecol. Lett. 9:853–869.

Moritz, C., J. L. Patton, C. J. Conroy, J. L. Parra, G. C. White, and S. R. Beissinger. 2008. Impact of a century of climate change on small-mammal communities in Yosemite National Park, USA. Science 322:261–264.

Nowak, R. M. 1999. Walker's mammals of the world. JHU Press, Baltimore, Maryland.

Oliveira, F. B., A. Porto, and G. Marroig. 2009. Covariance structure in the skull of Catarrhini: a case of pattern stasis and magnitude evolution. J. Hum. Evol. 56:417–430.

Ozgul, A., D. Z. Childs, M. K. Oli, K. B. Armitage, D. T. Blumstein, L. E. Olson, S. Tuljapurkar, and T. Coulson. 2010. Coupled dynamics of body mass and population growth in response to environmental change. Nature 466:482–485.

Paradis, E., J. Claude, and K. Strimmer. 2004. APE: analyses of phylogenetics and evolution in R language. Bioinformatics 20:289–290.

Patterson, B. D. 1980. A new subspecies of *Eutamias quadrivittatus* (Rodentia: Sciuridae) from the Organ Mountains, New Mexico. J. Mammal. 61:455–464.

———. 1983. On the phyletic weight of mensural cranial characters in chipmunks and their allies (Rodentia: Sciuridae). Fieldiana Zool. 20:1–24.

Pie, M. R., and J. S. Weitz. 2005. A null model of morphospace occupation. Am. Nat. 166:E1–E13.

Porto, A., F. B. Oliveira, L. T. Shirai, V. de Conto, and G. Marroig. 2009. The evolution of modularity in the mammalian skull I: morphological integration patterns and magnitudes. Evol. Biol. 36:118–135.

PRISM Climate Group. 2004. Oregon State University, Oregon.

Prôa, M., P. O'Higgins, and L. R. Monteiro. 2013. Type I error rates for testing genetic drift with phenotypic covariance matrices: a simulation study. Evolution 67:185–195.

R Core Team. 2014. R: a language and environment for statistical computing. R foundation for statistical computing, Vienna, Austria.

Reid, F. 2006. Peterson field guide to mammals of North America: fourth edition. Houghton Mifflin Harcourt, Boston, Massachusetts.

Reid, N., J. R. Demboski, and J. Sullivan. 2012. Phylogeny estimation of the radiation of western North American chipmunks (Tamias) in the face of introgression using reproductive protein genes. Syst. Biol. 61:44–62.

Roff, D. A. 1995. The estimation of genetic correlations from phenotypic correlations: a test of Cheverud's conjecture. Heredity 74:481–490.

Rowe, K. C., K. M. Rowe, M. W. Tingley, M. S. Koo, J. L. Patton, C. J. Conroy, J. D. Perrine, S. R. Beissinger, and C. Moritz. 2015. Spatially heterogeneous impact of climate change on small mammals of montane California. Proc. R Soc. B Biol. Sci. 282:20141857.

Schluter, D. 1996. Adaptive radiation along genetic lines of least resistance. Evolution 50:1766–1774.

———. 2000. The ecology of adaptive radiation. Oxford Univ. Press, Oxford.

Schluter, D., T. Price, A. O. Mooers, and D. Ludwig. 1997. Likelihood of ancestor states in adaptive radiation. Evolution 51:1699–1711.

Schmidt-Nielsen, K., F. R. Hainsworth, and D. E. Murrish. 1970. Countercurrent heat exchange in the respiratory passages: effect on water and heat balance. Respir. Physiol. 9:263–276.

Stayton, C. T. 2008. Is convergence surprising? An examination of the frequency of convergence in simulated datasets. J. Theor. Biol. 252: 1–14.

Sullivan, J., J. R. Demboski, K. C. Bell, S. Hird, B. Sarver, N. Reid, and J. M. Good. 2014. Divergence with gene flow within the recent chipmunk radiation (Tamias). Heredity 113:185–194.

Sutton, D. A., and B. D. Patterson. 2000. Geographic variation of the western chipmunks Tamias senex and T. siskiyou, with two new subspecies from California. J. Mammal. 81:299–316.

Van Valkenburgh, B., J. Theodor, A. Friscia, A. Pollack, and T. Rowe. 2004. Respiratory turbinates of canids and felids: a quantitative comparison. J. Zool. 264:281–293.

Voje, K. L., and T. F. Hansen. 2013. Evolution of static allometries: adaptive change in allometric slopes of eye span in stalk-eyed flies: evolution of static allometries. Evolution 67:453–467.

Wainwright, P. C., and S. M. Reilly, eds. 1994. Ecological morphology: integrative organismal biology. 1st ed. Chicago Univ. Press, Chicago.

Walsh, R. E., A. P. A. Assis, J. L. Patton, G. Marroig, T. E. Dawson, and E. A. Lacey. 2016. Morphological and dietary responses of chipmunks to a century of climate change. Glob. Change Biol. 22:3233–3252.

Wilson, D. E., and D. M. Reeder. 2005. Mammal species of the world: a taxonomic and geographic reference. JHU Press, Baltimore, Maryland.

Yom-Tov, Y., and H. Nix. 1986. Climatological correlates for body size of five species of Australian mammals. Biol. J. Linn. Soc. 29:245–262.

Zelditch, M. L., D. L. Swiderski, H. D. Sheets, and W. L. Fink. 2004. Geometric morphometrics for biologists: a primer. 1st ed. Elsevier, San Diego.

Zeng, Z.-B. 1988. Long-term correlated response, interpopulation covariation, and interspecific allometry. Evolution 42:363–374.

Associate Editor: I. Dworkin
Handling Editor: J. Conner

Supporting Information

Additional Supporting Information may be found in the online version of this article at the publisher's website:

Table S1. Sample size by species, divided by sex (female= ♀, male=♂, Unknown =U) indicating the subspecies measured (and respective sample size) when appropriate and the factors controlled for prior to the analysis in the MANOVA model.

Table S2. Landmarks recorded from crania by using a 3D digitizer with description and anatomical reference

Figure S1. Rarefaction analyses plots showing the distribution of self-correlation between matrices (y-axis; left compared using Krzanowski and right using Random Skewers) estimated from the same population (*T. quadrimaculatus*) with different sample sizes (x-axis). The lower values observed for matrices estimated with fewer than 25 individuals shows that sample size impacts the similarity between matrices.

Table S3. Average vector correlations between V/CV matrices responses to 10,000 random selection vectors for each pairwise species comparison.

Table S4. Structural similarity for covariance matrix based on Krzanowski comparison method.

Figure S2. Linear regression between observed eigenvalues coefficient of variation (C.V.) and sample size used on covariance matrix estimation (r^2=0.14, p=0.052).

Figure S3. Rarefaction analyses plot showing the distribution of eigenvalues coefficient of variation (estimated from the same population (*T. quadrimaculatus*) with different sample sizes (x-axis).

Table S5. Comparisons by Random Skewers and Krzanowski of ancestral **W**matrices (nodes displayed on the right) estimated using a weighted by sample size procedure or without considering sample sizes.

Table S6. Eigenvectors for the first ten principal components extracted from the pooled-within-groups morphological matrix (**W**-matrix for the *Neotamias* clade).

Figure S4. Regression test plots for each node in the phylogeny.

Figure S5. On the left phylogenies displaying the strength of selection estimates reconstructed using different reconstruction algorithms (maximum likelihood, squared parsimony and linear parsimony), with increasing values represented from light blue to dark blue/black colors.

Table S7. Projection of species means on the first principal component (PC1) and Centroid size means per species.